Hindawi
International Journal of Antennas and Propagation
Volume 2019, Article ID 6098014, 11 pages
https://doi.org/10.1155/2019/6098014

Research Article

Design of a Multiple Band Vehicle-Mounted Antenna

Yong Cheng, Jing Lu, and Can Wang

College of Electronic and Optical Engineering & College of Microelectronics, Nanjing University of Posts and Telecommunications, Nanjing 210003, China

Correspondence should be addressed to Yong Cheng; chengy@njupt.edu.cn

Received 14 August 2019; Revised 13 September 2019; Accepted 23 November 2019; Published 16 December 2019

Academic Editor: Paolo Baccarelli

This paper designs a vertically polarized, horizontal, omnidirectional vehicle antenna for the mobile communication band, covering the available frequency bands of the wireless sensor network and 5G. The antenna is composed of semi-T monopole and semicone monopole, which are placed vertically on the metal plate, especially suitable for being mounted on top of a car. T-branch mainly works at low frequency, and cone branch mainly works at high frequency. The cone branch adopts tapered structure in order to improve the impedance matching of antenna and increase the bandwidth of antenna. The antenna can be miniaturized by cutting the antenna in half. The operating frequencies of the antenna are 770 MHz–1000 MHz and 1.7 GHz–3.78 GHz which can cover multiple wireless system bands, including GSM, LTE, and 5G.

1. Introduction

The mobile communication band mainly includes three frequency bands: 824 MHz–960 MHz, 1710 MHz–2690 MHz, and 3.4 GHz–3.6 GHz. Microstrip antennas are the best choice for multifrequency miniaturized antennas due to their small size, light weight, easy integration, and low profile. Conventional monopole is not easy to install on the top of the vehicle due to its large size. Printed monopole antennas [1, 2] overcome the volume defects and bandwidth defects of conventional monopole antennas by printing conventional monopole antennas on a dielectric substrate. It has similar structural characteristics and performance advantages as microstrip antennas. Therefore, it is widely used in mobile communication band antennas [3, 4].

Nowadays, in order to implement a variety of wireless mobile communication systems, it is necessary to install a plurality of vehicle antennas on the vehicle [5], and each antenna is preferably multifrequency [6, 7]. At the same time, in order to be better integrated in the vehicle, the vehicle antenna needs to be miniaturized. After 2020, the 5G system will be put into commercial use, which puts new requirements on the frequency band of the antenna. It is necessary not only to add new frequency bands to the original vehicle antennas, but also to maintain the high performance of the vehicle antennas. Therefore, while maintaining the excellent performance of the vehicle antenna, it does not affect the aesthetics of the vehicle, which puts high demands on the miniaturization design and multifrequency design of the antenna.

In [8], the paper presents the design of a long-term evolution (LTE) antenna and its integration on the 3D surface of the mounting compartment of an automotive roof-top antenna, using molded interconnect device (MID) technology. A conformal and optimized two antenna system is introduced and discussed. A prototype realized by MID laser direct structuring (LDS) is presented. It is targeted to operate at LTE 800 MHz (791–862 MHz), 1800 MHz (1710–1880 MHz), and 2600 MHz (2520–2690 MHz). In [9], the integration of a two-antenna MIMO system for usage in worldwide LTE networks into a conventional automotive roof top antenna is discussed. For a potential worldwide use of the antenna modules, the following three major frequency bands for LTE should be covered: 698 MHz to 960 MHz, 1710 MHz to 2170 MHz, and the highest frequency band covers 2500 MHz to 2690 MHz. In [10], a low-profile printed antenna is proposed, covering wireless standards in a wide frequency range (698–2690 MHz). Multiple monopole antennas are printed on the same compact substrate. A tapered profile and a thin slot have been introduced to achieve good

impedance matching, especially at higher frequencies. In [11], a novel compact broadband monopole antenna inspired by a Vivaldi antenna is presented. The wideband antenna covers LTE700, GSM850, GSM900, DCS1800, PCS1900, WCDMA2100, Bluetooth, WiMAX2350, WLAN2400, and LTE2600, with a size reduction length of 30% over conventional monopole antennas. In contrast to traditional designs using Vivaldi antennas, a compact design with omnidirectional radiation pattern is proposed. The proposed design is perpendicularly mounted to a ground plane, being then suitable for mobile communications in vehicular applications. In [12], anovel compact 3D antenna operating at LTE, GSM, and UMTS frequency bands (790–2690 MHz) is proposed. The size of the antenna is $50 \times 50 \times 30\ \text{mm}^3$. A planar inverted-F antenna is designed to cover the lower frequency band, while an integrated folded monopole adds higher frequency resonances.

The wireless communication of the sensor network can be used in the 868 MHz, 908 MHz, and 2.4 GHz bands. This paper presents the design of a vertically polarized, horizontal, omnidirectional vehicle antenna for the mobile communication band. Some parts of the tapered branch are cut to improve the impedance matching and increase the bandwidth. By splitting the antenna in two, the size is miniaturized. The bandwidth of the two bands is 240 MHz (720 MHz–960 MHz) and 2.4 GHz (1.6 GHz–4 GHz), covering the available frequency bands of the wireless sensor network and 5G. Compared with the antennas mentioned in the references, the antenna proposed in this paper has higher gain and wider bandwidth than similarly sized antennas.

2. Structural Design of the Two-Branch Vehicle Antenna

The antenna of the mobile communication band designed in this paper consists of a dielectric plate, a semi-T monopole, a semiconical monopole, and a metal floor. The structure is shown in Figure 1. The gray part indicates the dielectric substrate, the yellow part indicates the metal radiating antenna, the red part indicates the feeding part, and the antenna is vertically mounted on the metal floor of 300 mm ∗ 300 mm. The antenna was printed on a dielectric substrate made of FR4 ($\varepsilon_r = 4.4$, $\tan\ \delta = 0.02$) with the thickness of 1.6 mm. The coaxial line was fed, and the impedance matching was set to 50 Ohm. A metal radiating element is etched on the dielectric substrate. The radiating element is composed of a T-shaped monopole branch and a tapered monopole branch. The antenna size is 70 mm ∗ 60 mm, wherein the T-shaped monopole branch mainly works in mobile communication. In the low-frequency band, the tapered monopole branch mainly works in the high-frequency band of mobile communication, and the impedance design is improved by the gradual design to broaden the bandwidth. At the same time, in order to reduce the size of the antenna, the antenna is halved without substantially changing the current distribution to form a final semi-T-shaped monopole branch and a semiconical monopole branch, the antenna size being 70 mm ∗ 30 mm ∗ 1.6 mm. The ground of the antenna is 300 mm ∗ 300 mm.

The size of the printed monopole is optimized by the HFSS electromagnetic simulation software to obtain the final dimensions, as shown in Table 1.

3. Design Process of the Two-Branch Vehicle Antenna

In order to illustrate the design idea of planar monopole, Figure 2 shows the evolution of antenna. The goal of the antenna in this paper is to support the mobile communication frequency band, namely low frequency as 824 MHz–960 MHz and high frequency as 1710 MHz–2690 MHz and 3.4 GHz–3.6 GHz. As shown in Figure 2(a), the T-shaped monopole works at low frequency. To make the antenna work at high frequencies, two branches are introduced at the sides of the T-shaped monopole. Figure 3 compares the performance of a T-shaped monopole antenna and the antenna with two branches. As shown in Figure 3, the improved antenna can work at 0.78 GHz and 2.66 GHz.

In order to make the working bandwidth of the antenna wider, the bottom of the two branches is designed as a tapered structure, as shown in Figure 2(b). Figure 4 compares the performance of this tapered antenna and the ordinary antenna of Figure 2(b), and it is found that this tapered structure greatly improves the impedance matching of the antenna. From 1.7 GHz–3.95 GHz, the S11 is lower than −10 dB. The antenna size is 60 mm ∗ 70 mm.

It can be found that the antenna shown in Figure 2(c) is a symmetrical antenna, and the shape is not only symmetrical but also the current distribution is substantially symmetrical. Cutting the antenna in half does not substantially change the current distribution. Therefore, in order to reduce the size of the antenna, the antenna is cut in half and the rest is unchanged, and finally the model antenna shown in Figure 2(d) is obtained.

Figure 5 shows that the bandwidth of the antenna before halving is 0.75 GHz–1 GHz and 1.7 GHz–3.95 GHz. After halving, the bandwidth of the antenna is 0.77 GHz–1 GHz and 1.7 GHz–3.78 GHz. Before and after halving, the antenna bandwidth has been reduced, but still covers the AMPS, GSM900, GSM1800, TD-LTE, and 5G mobile communication bands. Finally, the antenna size is 30 mm ∗ 70 mm.

4. Simulation Analysis of the Two-Branch Vehicle Antenna

In this paper, the current of the antenna radiating patch is simulated by HFSS and analyzed. Figure 6 shows the surface current distribution before and after the antenna is bisected at 0.9 GHz, 2.0 GHz, and 3.5 GHz. The current distribution on the surface of the antenna after halving is similar to the current distribution in the right half of the antenna before halving. Since the antenna structure before halving is symmetrical, the excitation of the antenna to the

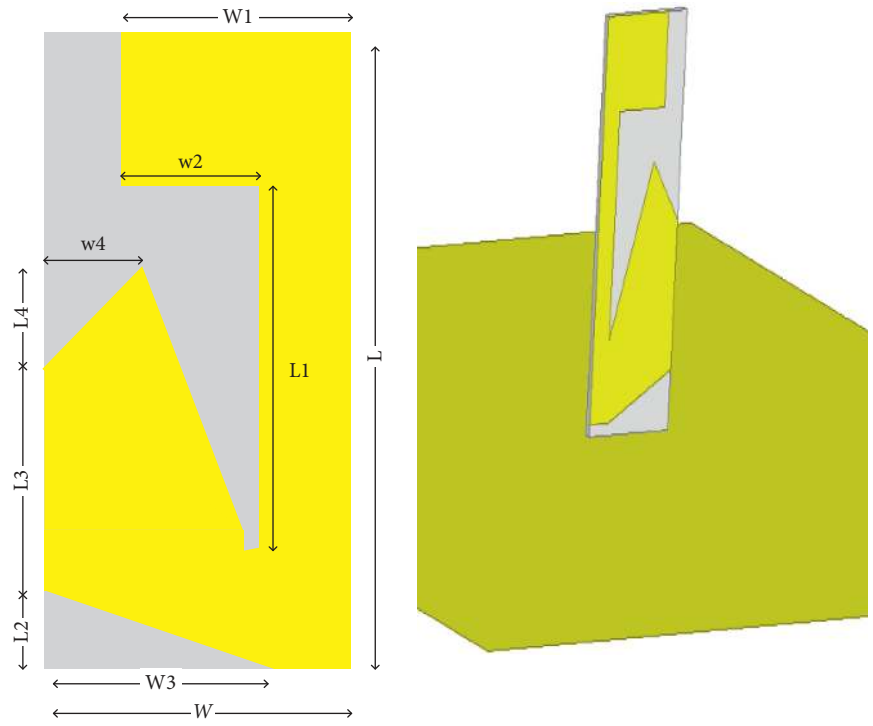

Figure 1: Structure of the two-branch vehicle antenna: (a) planar structure diagram; (b) stereoscopic structure diagram.

Table 1: Antenna size parameters.

Parameters	Values (mm)
L	70
L1	35
L2	8
L3	25
L4	10.09
W	30
W1	22
W2	13.5
W3	23
W4	10.13

symmetrical structure is uniform, so the left half of the antenna before halving does not generate current distribution on the right half (miniature structure).

It can be seen from Figure 6 that the frequency is different and the current of the antenna radiating patch is also different. When the low frequency is 0.9 GHz, the surface current of the monopole patch mainly flows in the $-z$ direction on the T-shaped structure, and the current of a small amount of the tapered portion also flows in the $-z$ direction. The intermediate frequency 2G is mainly contributed by the lower part of the T-shaped structure and the lower part of the tapered structure, and the current flows in the −z direction. At the high frequency of 3.5 G, the antenna current is concentrated in the tapered portion, and the current flows in the $+z$ direction, which is opposite to the direction of the low-frequency current. The abovementioned current distribution shows that the low frequency of the antenna mainly has T-shaped monopole generation, the intermediate frequency is produced by the gradient cone and the T-shaped monopole, and the high frequency is mainly generated by the gradient cone. These current distributions are basically consistent with the design flow of the antenna, which proves that the design idea is correct. It should be noted that the currents in the X direction are canceled by the antennas before halving, and the antennas after halving are not.

Figure 7 shows the radiation pattern before and after the antenna is split in half. Since the current distribution of the antenna is basically unchanged before and after halving, the antenna should have similar radiation characteristics. It can be seen from the figure that at 0.9 GHz, the radiation pattern of the antenna before and after the halving is completely consistent; at 2 GHz, the radiation pattern of the antenna is basically the same; and at 3.5 GHz, after antenna is cut, the figure appears larger. But on the E-plane, the maximum radiation pattern of the antenna is similar. On the H-plane, the radiation pattern of the antenna in the $+z$ direction is basically the same. Therefore, at low frequency and intermediate frequency, the halving technique has essentially no effect on the antenna pattern. It only affects the antenna pattern at high frequency.

It is found in Figure 8 that at low frequency, the antenna gain after halving is lower than before; at high frequency, the antenna gain after halving is higher than before. Especially at 3.6 GHz, the antenna gain is enhanced by 3.28 dBi. Before halving, the antenna has a maximum gain of 5.52 dBi at 3.4 GHz. After halving, the antenna has a maximum gain of

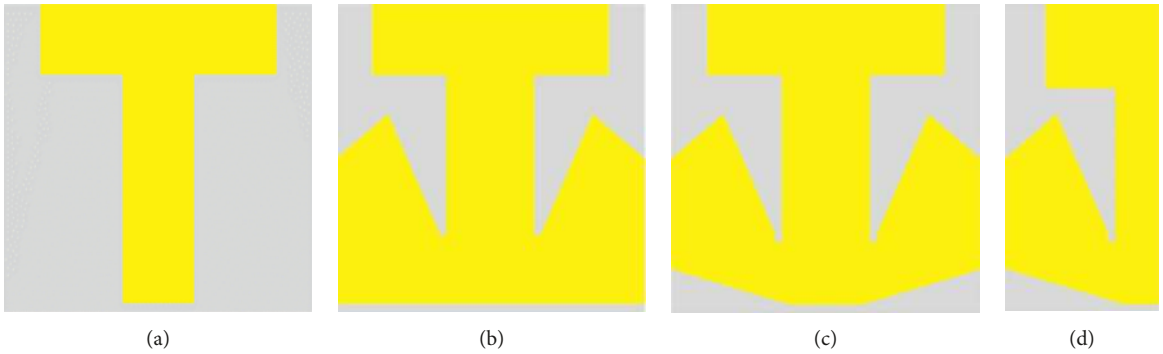

Figure 2: Evolutionary structure of printed monopole: (a) T-shaped monopole; (b) two-branch monopole; (c) tapered two-branch monopole; (d) tapered two-branch monopole after cutting it in half.

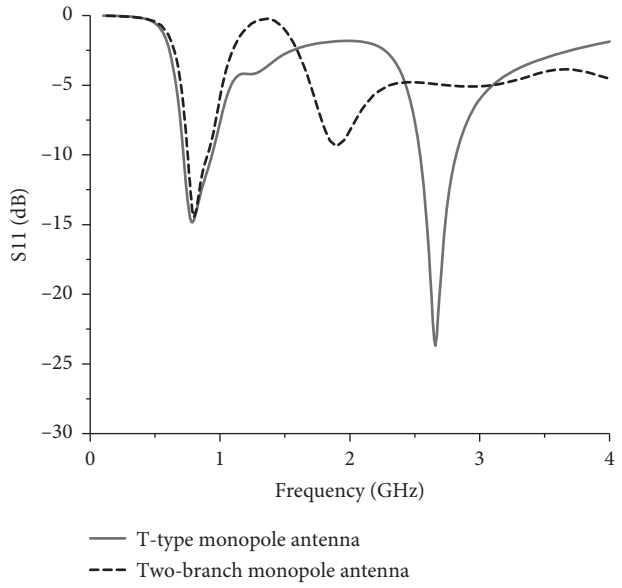

Figure 3: Comparison of a T-shaped monopole antenna and two-branch monopole antenna.

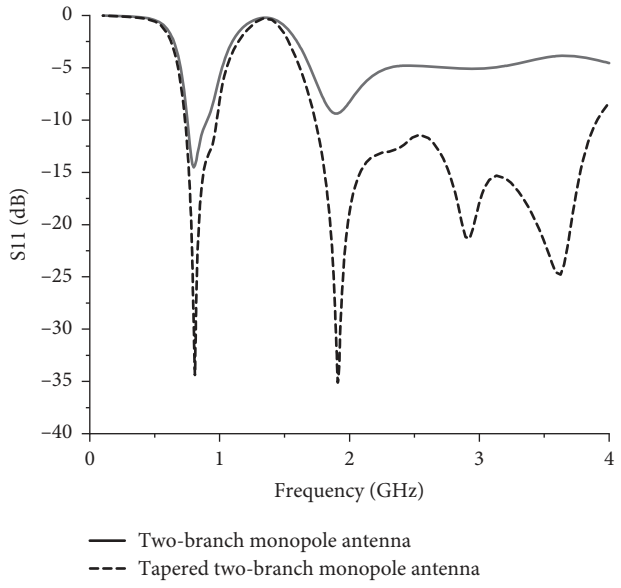

Figure 4: Comparison of two-branch monopole antenna and tapered two-branch monopole antenna.

7.99 dBi at 3.6 GHz. The dimension of the ground floor is unchanged and the size of the monopole is reduced, so that the front-to-back ratio is increased. In summary, it can be clearly proved that for the two-branch vehicle antenna, halving is a successful method to reduce the size of the antenna. The antenna satisfies the bandwidth requirement and supports omnidirectional radiation to meet the gain requirements.

5. Processing and Measurement of the Two-Branch Vehicle Antenna

Figure 9 shows the actual antenna processed according to the antenna size in Table 1. The antenna uses FR4 as the dielectric board, and the substrate is brushed with tin. The measurement data tested by Agilent's vector network analyzer is compared with the simulation data, as is shown in Figure 10. As can be seen, compared with the simulation, the entire frequency band of the processed antenna is shifted to the left. This is caused by the processing error and the instability of the dielectric substrate. With a reflection coefficient of −10 dB as the standard, the working band of the processed antenna is 720 MHz–960 MHz and 1.6 GHz–4 GHz, which can cover AMPS, GSM900, GSM1800, LTE, and 5G bands.

The far field characteristics of the antenna can be seen by measuring the normalized pattern and gain of the antenna through the microwave darkroom. The normalized pattern on the two vertical planes of the E and the H is used to show the directivity of the antenna in the far field. Figure 11 shows a comparison of the normalized pattern of simulation and measurement of the antenna on the E and H planes at three frequencies (0.9 GHz, 2.5 GHz, and 3.5 GHz). The H-plane of the antenna has good omnidirectionality at both 0.9 GHz and 2.5 GHz, satisfying the omnidirectional radiation requirement of the vehicle antenna. At 0.9 GHz, the antenna has an approximate "8" shape on the E-plane, which is similar to a half-wave dipole antenna. But, due to the

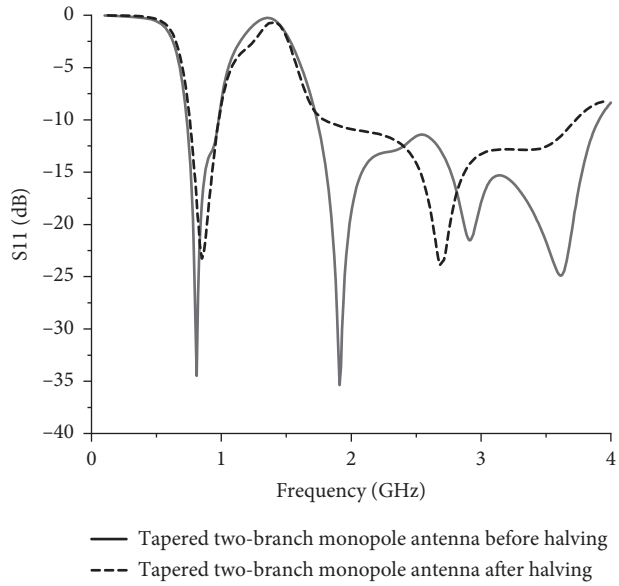

Figure 5: Comparison of a tapered two-branch monopole antenna before and after halving.

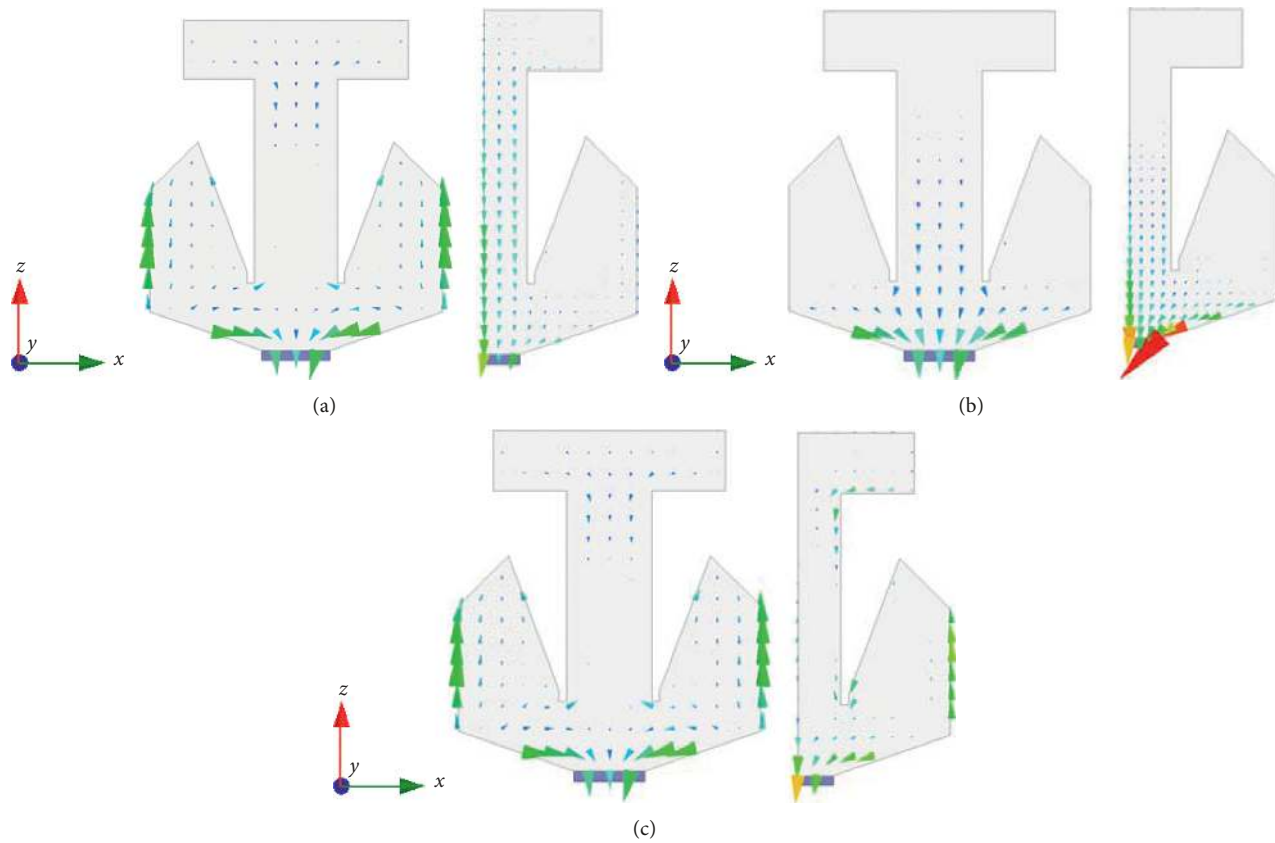

Figure 6: Effect of halving on the surface current distribution of the antenna at different frequencies. (a) 0.9 GHz, (b) 2 GHz, and (c) 3.5 GHz.

reflection of floor, the main radiation direction of the antenna is no longer strictly 90 degrees. It is at 45 degrees. At 2.5 GHz, the measured pattern also has an upward tilting trend compared with the simulated E-plane radiation pattern, but the main radiation direction is more inclined to 90 degrees. At 3.5 GHz, the E-plane radiation pattern has

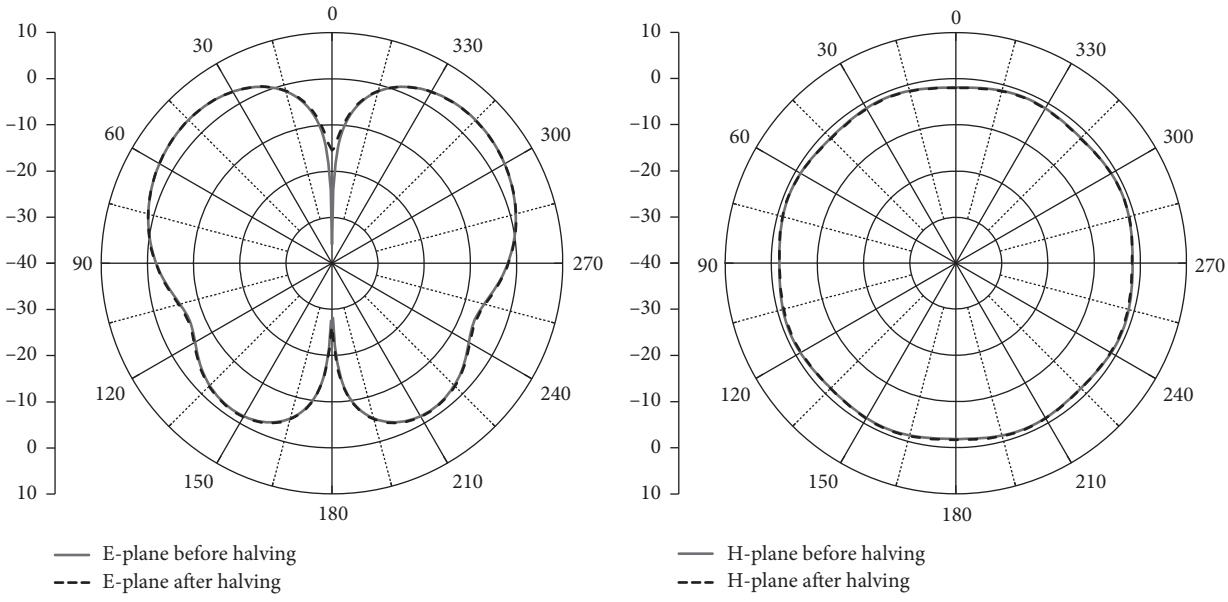

(a)

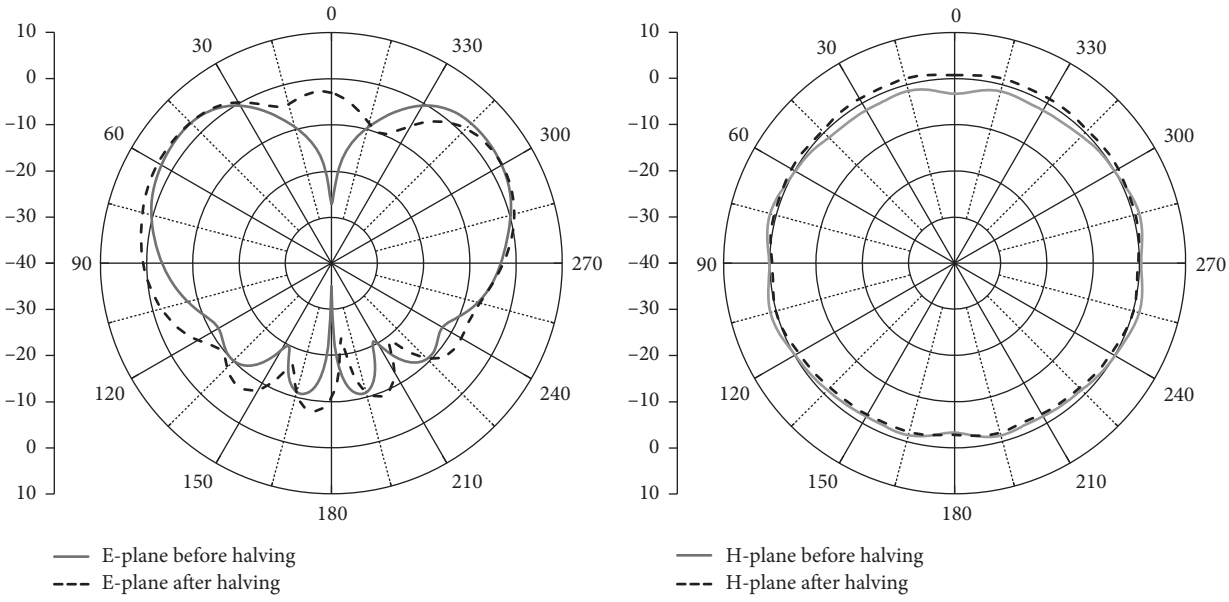

(b)

Figure 7: Continued.

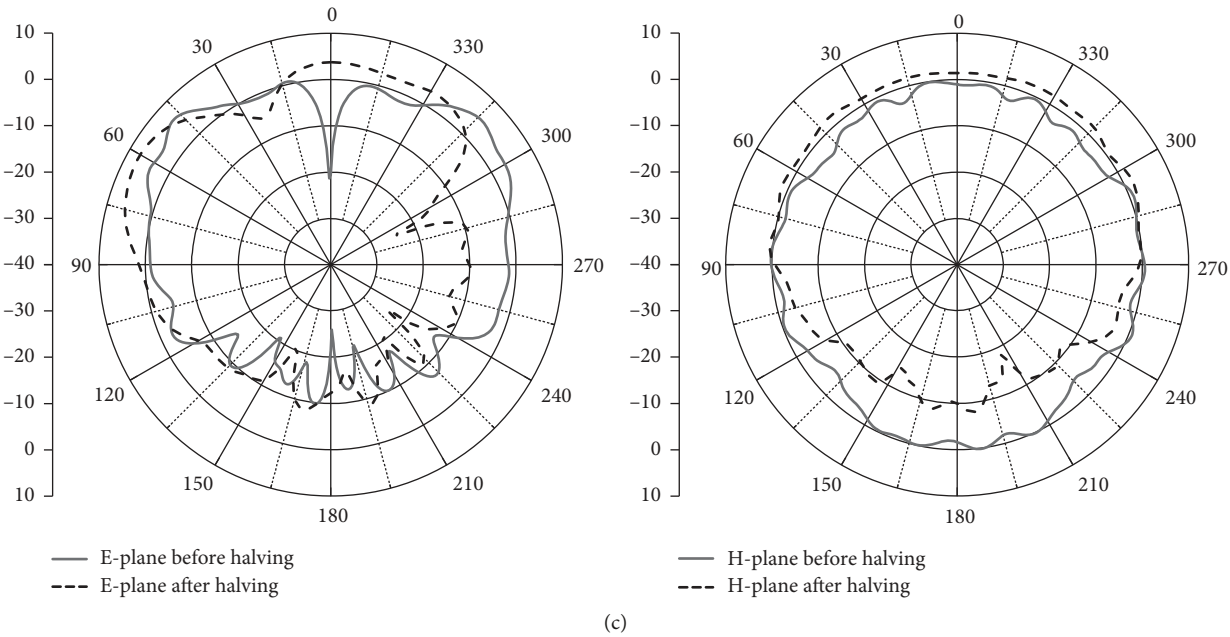

(c)

Figure 7: Effect of halving on radiation pattern at different frequencies. (a) 0.9 GHz, (b) 2 GHz, and (c) 3.5 GHz.

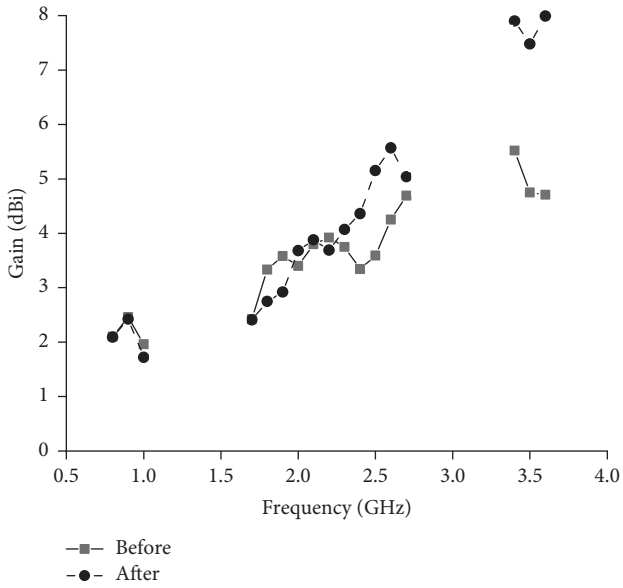

Figure 8: The gain of the antenna before and after halving.

Figure 9: The two-branch vehicle antenna.

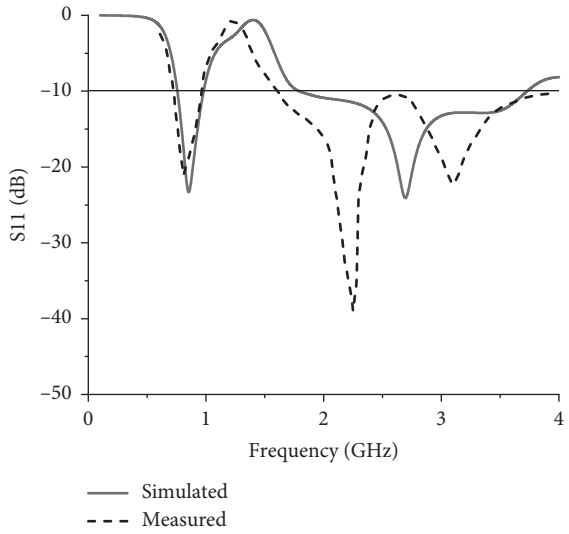

Figure 10: The simulation and measurement of two-vehicle antennas.

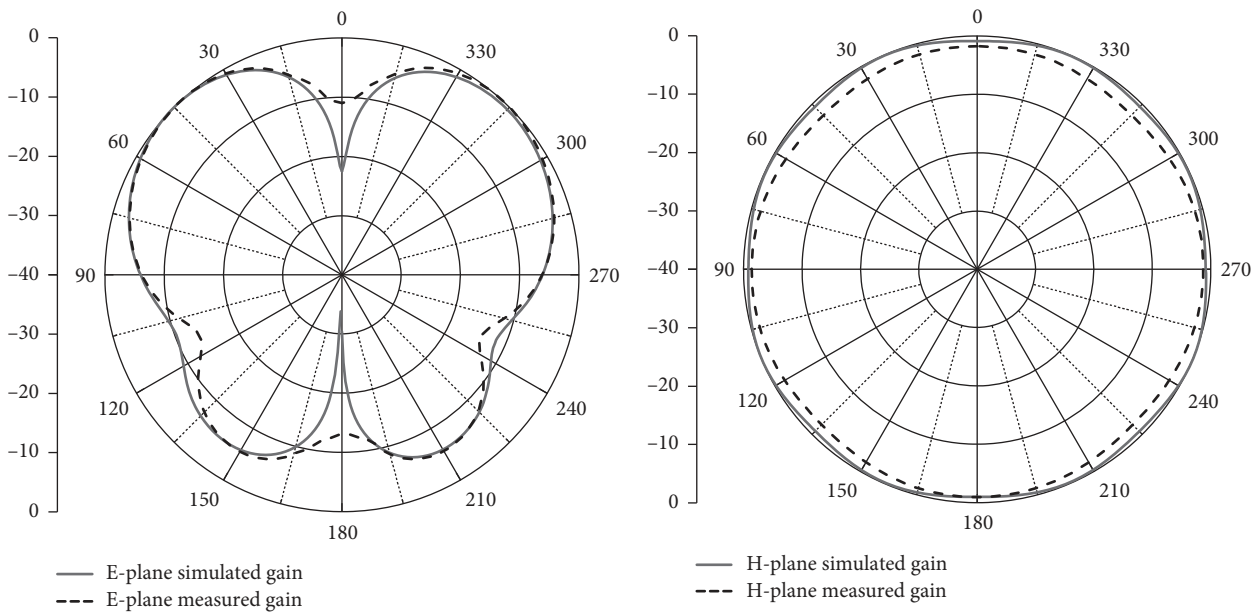

(a)

Figure 11: Continued.

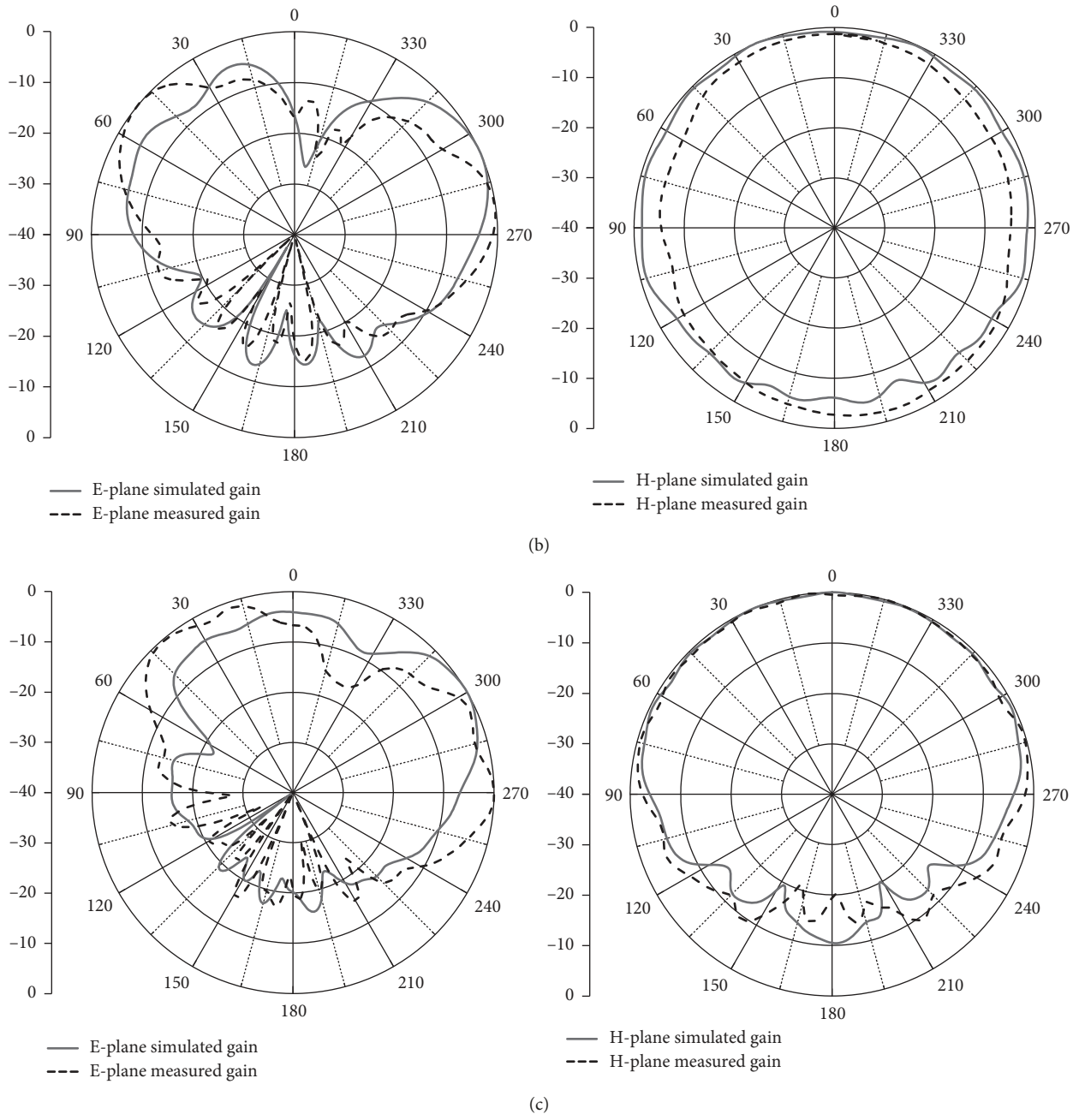

Figure 11: Simulated and measured gain of the two-branch vehicle antenna at different frequencies. (a) 0.9 GHz; (b) 2 GHz; (c) 3.5 GHz.

obvious side lobes and the main lobe is enhanced, so the gain of the antenna at the high frequency is larger than that at the low frequency.

Figure 12 shows the measured gain of the antenna. The gain of the antenna at 0.9 GHz is 3.54 dBi, the gain at 3.5 GHz is 3.52 dBi, and the gain at 2.4 GHz is the largest at 5.89 dBi, which fully meets the gain requirements of the vehicle antenna.

In Table 2, we compared several similar antennas. From the table, we can see that the antenna proposed in this paper has higher gain than the similar size antenna. Reference [10] has the similar size and gain, but the band is smaller than the antenna in this paper. Reference [11] has a higher gain, but its size is far beyond 70 mm.

6. Conclusion

A two-branch vehicle antenna has been designed with the requirements of the mobile communication band. The antenna is based on a monopole antenna and consists of a T-monopole and a tapered monopole placed vertically on a metal floor. Some parts of the tapered branch are cut to improve the impedance matching and to increase the bandwidth. The largest gain of the antenna is 5.89 dBi and

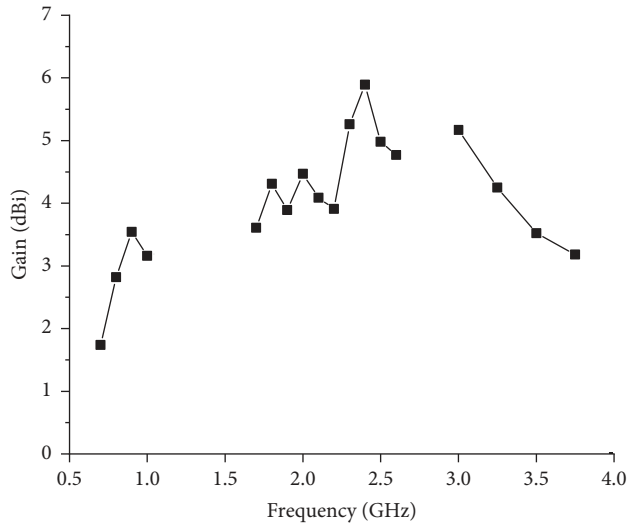

Figure 12: Measurement of the gain of the two-branch vehicle antenna.

Table 2: Comparison of similar antennas.

Antennas	Size: length ∗ width ∗ thickness (mm)	Band (MHz)	Frequency (MHz)	Gain (dBi)
Reference [10]	76 ∗ 25 ∗ 1.53	2000	700–2700	≥2
Reference [11]	125 ∗ 90 ∗ 0.81	1980	700/900/1800/2100/2500	3.64/3.54/5.21/5.54/6.42
Reference [12]	50 ∗ 50 ∗ 30	170/460/200	900/1800/2150/2600	—
Reference [13]	53 ∗ 50 ∗ 2	262/1230	850/1700	5/6
Reference [14]	401.7 ∗ 245∗0.8	500	180/430/650	1.9/7.6/7.1
This work	70 ∗ 30 ∗ 1.6	240/2400	900/2400/3500	3.54/5.89/3.52

the bandwidths of the two bands are 240 MHz (720 MHz–960 MHz) and 2.4 GHz (1.6 GHz–4 GHz), which are wider than those of several similar antennas. By halving the antenna, the size of the monopole is only 70 mm ∗ 30 mm ∗ 1.6 mm.

Data Availability

The data used to support the findings of this study are included within the article.

Conflicts of Interest

The authors declare that they have no conflicts of interest.

Acknowledgments

This work was supported in part by the National and Local Joint Engineering Laboratory of RF Integration and Micro-Assembly Technology (grant no. KFJJ20170206), Research Project of Nanjing University of Posts and Telecommunications (no. 208035), and in part by the University of Macau (grant no. CPG2019-00024-FST).

References

[1] R. Zaker and A. Abdipour, "A very compact ultrawideband printed omnidirectional monopole antenna," *IEEE Antennas and Wireless Propagation Letters*, vol. 9, pp. 471–473, 2010.

[2] Y. Zhu, F.-s. zhang, C. Lin, Y.-C. Jiao, and R. Zou, "Design of a compact dual-band printed monopole antenna for WLAN applications," in *Proceedings of the 9th International Symposium on Antennas, Propagation and Em Theory*, pp. 1–3, Guangzhou, China, 2010.

[3] M. S. Sharawi, Y. S. Faouri, and S. S. Iqbal, "Design of an electrically small meander antenna for lte mobile terminals in the 800 MHz band," in *Proceedings of the 2011 IEEE GCC Conference and Exhibition (GCC)*, pp. 213–216, Dubai, UAE, February 2011.

[4] I. Goncharova and S. Lindenmeier, "A high efficient automotive roof-antenna concept for LTE, DAB-L, GNSS and SDARS with low mutual coupling," in *Proceedings of the 2015 9th European Conference on Antennas and Propagation (EuCAP)*, pp. 1–5, Lisbon, Portugal, April 2015.

[5] T. Mahler, J. Kowalewski, L. Reichardt, and T. Zwick, "Realization of a synthesized compact automotive roof-top LTE antenna," *Electronics Letters*, vol. 45, pp. 305-306, 2013.

[6] D. Garrido Lopez, M. Ignatenko, and D. S. Filipovic, "Low-profile tri-band inverted-F antenna for vehicular applications in HF and VHF bands," *IEEE Transactions on Antennas and Propagation*, vol. 63, no. 11, pp. 4632–4639, 2015.

[7] S. Verma and Kumar, "A compact printed antenna for triple-band WiMAX/WLAN applications," *IEEE Antennas & Wireless Propagation Letters*, vol. 12, pp. 1536–1225, 2013.

[8] A. Friedrich, B. Geck, O. Klemp, and H. Kellermann, *On the Design of a 3D LTE Antenna for Automotive Applications Based on MID Technology*, in *Proceedings of the 2013 European Microwave Conference*, pp. 640–643, Nuremberg, Germany, 2013.

[9] A. Thiel, L. Ekiz, O. Klemp, and M. Schultz, "Automotive grade MIMO antenna setup and performance evaluation for LTE-communications," in *Proceedings of the 2013 International Workshop on Antenna Technology (iWAT)*, pp. 171–174, Karlsruhe, Germany, 2013.

[10] A. Michel, P. Nepa, M. Gallo, I. Moro, A. P. Filisan, and D. Zamberlan, "Printed wideband Antenna for LTE-band Automotive applications," *IEEE Antennas and Wireless Propagation Letters*, vol. 16, pp. 1245–1248, 2017.

[11] D. V. Navarro, F. Carrera, M. Ferrando et al., "Compact wideband Vivaldi monopole for LTE mobile communications," in *Proceedings of the 2013 IEEE Antennas and Propagation Society International Symposium (APSURSI)*, vol. 14, pp. 1068–1071, Orlando, FL, USA, July 2015.

[12] V. Franchina, A. Michel, P. Nepa et al., "A 3D LTE antenna for vehicular applications," in *Proceedings of the 2017 IEEE International Symposium on Antennas and Propagation & USNC/URSI National Radio Science Meeting*, pp. 637-638, San Diego, CA, USA, July 2017.

[13] I. Goncharova and S. Lindenmeier, "A high-efficient 3-D Nefer-antenna for LTE communication on a car," in *Proceedings of the IEEE European Conference on Antennas and Propagation*, pp. 3273–3277, The Hague, Netherlands, 2014.

[14] K. Iigusa, F. Kojima, and H. Yano, "A fin type wideband bent monopole antenna closed to L-shape grounded plate for vehicular communications," in *Proceedings of the 2015 9th European Conference on Antennas and Propagation (EuCAP)*, pp. p1–2, Lisbon, Portugal, April 2015.